Diffusion NMR as a New Method for the Determination of the Gel Point of Gelatin

Torsten Brand,[†] Sven Richter,*[,‡] and Stefan Berger*[,†]

Institute of Analytical Chemistry, University of Leipzig, Linnéstrasse 3, D-04103 Leipzig, Germany, and Physical Chemistry of Polymers, Dresden University of Technology, Mommsenstrasse 13, D-01062 Dresden, Germany

Received: May 15, 2006; In Final Form: June 22, 2006

The gelation of gelatin has been investigated using pulsed field gradient (PFG) NMR. For the first time, diffusion results have been used to determine the gelation point, which is indicated by a minimum in the self-diffusion coefficient of the free polymer fraction vs temperature. Biexponential analysis of the diffusion decay data allowing the diffusion of free and network-bound gelatin to be determined separately has been applied to provide an extended insight into the gelation process. Low-amplitude oscillatory shear rheology and time-resolved dynamic light scattering (DLS) as classical polymer characterization methods were applied as control experiments. All three methods yielded a gelation temperature of 24−25 °C for the cooling regime. Hysteresis effects could also be observed.

Introduction

Gelatin is a biopolymer made from collagen through a hydrolysis process. The native conformation of collagen molecules is a triple helix formed by three individual molecular strands held together by interchain hydrogen bonding.[1,2] Gelatin dissolved in water at temperatures above the melting temperature consists of flexible individual random coils in solution. On cooling below the melting temperature, ordered structures of the gelatin molecules are formed. It has been shown that the ordered gelatin structures have the same conformation as collagen.[1,2] Gelatin molecules partially revert to the ordered helical collagen-like sequences, separated along the gelatin molecular chain by peptide residues in the disordered random coil conformation. While the coil−helix reversion is predominantly intramolecular through a back refolding of the single chains at very low concentrations (∼0.01−0.1 wt %), it becomes increasingly intermolecular as concentration is raised. This leads to gelation at concentrations above 0.5−1 wt % caused by the formation of an infinite network of intermolecularly connected molecules. The gelation of gelatin was found to obey the general scheme of percolation, and gelatin exhibits a gel point that depends only on the amount of renatured helices (fraction of reacted bonds).[3] The elastic moduli versus helix amount follows the predicted scaling laws. At the gel point, the helix amount is only a few percent.[3]

The applications of gelatin in food, pharmaceutical, and photographic industries are directly attributed to its coil−helix transition. The study of this physical gelation process has attracted considerable research attention for many years.[1−11] The gelation temperature is the primary indicator of gel formation.

Diffusion NMR has been applied to a variety of studies in organic, inorganic, and organometallic chemistry including problems related to the characterization of molecules and complexes with respect to size and shape, and it has been used for the investigation of intermolecular interactions.[12−17] In a polymeric gelling system pulsed field gradient (PFG) NMR has been applied previously to study anomalous diffusion, which can be caused by the presence of internal barriers. This results in a mean square displacement $\langle z^2(\Delta)\rangle$ that is no longer proportional to the diffusion time Δ.[18] In the gelatin system, anomalous diffusion has been investigated by dynamic light scattering (DLS) experiments.[19]

For NMR to be applicable to the determination of sol−gel transitions, it should have the principal advantage vs rheology that a hysteresis could be detected easily. NMR measurements, as well as DLS, can be performed continuously through the transition temperature (cooling and heating), which is difficult in rheology, and they do not disturb the system by introducing shear forces. Previously, NMR investigations for the monitoring of gelation processes in other thermoreversible gelling systems used longitudinal (T_1) and transversal (T_2) relaxation times as observables.[20,21] In some studies, the solvent water has been used as a reporter molecule for monitoring gelation.[21,22]

Experimental Methods

Gelatin (high gel strength, 250 g Bloom) from porcine skin was used as received from Fluka. A 9:1 (v/v) mixture of H_2O and D_2O (the typical solvent in biomolecular NMR) was used in all experiments for reasons of comparability. The gelatin solution (40 g/L) was obtained by immersion of gelatin in the solvent for 15 min, dissolution at 60 °C under stirring for 1 h, and subsequent filtration through a 0.45 μm membrane filter. Molecular characterization by static light scattering yielded a weight-average molecular weight of $M_W = 85\,000$ g mol^{-1} and a radius of gyration of $R_g = 28$ nm.

Low-amplitude oscillatory shear rheology experiments were carried out using a Fluids Spectrometer RFS 2 from Rheometric Scientific with a Couette system (cup diameter 34 mm, bob diameter 32 mm, bob length 33.3 mm). Applied strains ranged from 150% (to provide sufficient torque response in the liquid state) to 50% (to avoid breakdown of the formed gel structure near the gelation threshold). Linear viscoelastic behavior of the

* To whom correspondence should be addressed. Phone: (+49) 341-9736101. Fax: (+49) 341-9736115. E-mail: stberger@rz.uni-leipzig.de (S.B.). Phone: (+49) 351-46332492. Fax: (+49) 351-46337122. E-mail: sven.richter@chemie.tu-dresden.de (S.R.).

[†] University of Leipzig.

[‡] Dresden University of Technology.

10.1021/jp062960z CCC: $33.50
Published on Web 07/26/2006

material was proven by strain-sweep experiments using different constant frequencies. A solution volume of 17 mL was used here for the measurements. The cooling regime was performed as described for the DLS.

Furthermore, it is well-known that shearing of the sample can induce or impede thermoreversible gelation; see, e.g., refs 3 and 23. Therefore, we performed several small-amplitude oscillatory shear experiments in the rheometer on the present system to check this effect. In our studies parameters such as different shear strains, shear history, thermal sample history, and aggregation did not influence the gelation temperature of 25 °C in any case. As an example, a direct jump to 25 °C followed by an equilibration period at this temperature (without performing any previous rheological experiments), also leads to a power law in G' and G'' at this temperature.

DLS experiments were performed at a scattering angle of $\theta = 90°$ using an ALV/DLS/SLS-5000 laser light scattering spectrometer equipped with an ALV-5000/EPP multiple digital time correlator, with a helium−neon laser ($\lambda = 632.8$ nm) as the light source. A toluene bath was used for thermostating the sample (3 mL of solution in a test tube (diameter 10 mm)) within an error of ±0.1 °C. For monitoring the gelation process via the time−intensity correlation functions (TCFs), a cooling regime starting at 60 °C with 2−0.5 K steps downward was applied, allowing 15 min for equilibration at each temperature. An acquisition time of 10 min was used for each TCF, providing enough data points, especially at longer delay times. ALV correlator software was used to calculate mean relaxation times.

All NMR experiments were performed on a Bruker Avance 700 spectrometer equipped with a cryoprobe. For diffusion measurements the stimulated echo sequence[24] with a longitudinal eddy current delay (LED) (5 ms) was used. In the proton dimension of the diffusion experiments a sweep width of 14 ppm was used; 32 768 data points have been recorded in eight transients. After multiplication with an exponential function, Fourier transformation (FT) was applied to the free induction decays (FIDs). For diffusion encoding a diffusion time $\Delta = 150$ ms was used. Bipolar gradients (half-sine shape, 5 ms duration of individual pulses ($\delta = 10$ ms)) were employed with a strength varied linearly from 0.011 to 0.523 T m^{-1} in 10 steps. A gradient recovery delay of 50 μs and a 180° pulse of 16 μs were used, which resulted in a separation of the individual gradient pulses of the bipolar pairs of $\tau = 66$ μs.

The gradient calibration was performed by recording an image of the water distribution in an NMR tube additionally containing a Teflon disk with known thickness.[25] Applying the approach presented by Damberg et al.,[26] we checked if local differences of the gradients could influence our results. We recorded the diffusional decay of the residual HDO signal in a D_2O sample at 25 °C and used the literature value[27] for its diffusion coefficient ($D = 1.9 \times 10^{-9}$ m^2·s^{-1}) for the calculations. Fitting the data to eq 6 of ref 26, which includes two parameters g_{min} and g_{max} used to model a distribution of the gradient, does not yield significantly better results than using eq 6 of the present paper, which uses only one gradient strength for the whole sample. Therefore, uniform gradients (with a maximum strength of 0.56 T m^{-1}) are assumed for all calculations of diffusion coefficients.

The total time where transversal (T_2) relaxation is effective was 20.2 ms. The transversal relaxation time of the investigated species, which was estimated using the Carr−Purcell−Meiboom−Gill (CPMG) sequence,[28] exceeds 20 ms by far. Thus all species will contribute to the apparent diffusion coefficients, although different relaxation times of different species can introduce some "weighting".

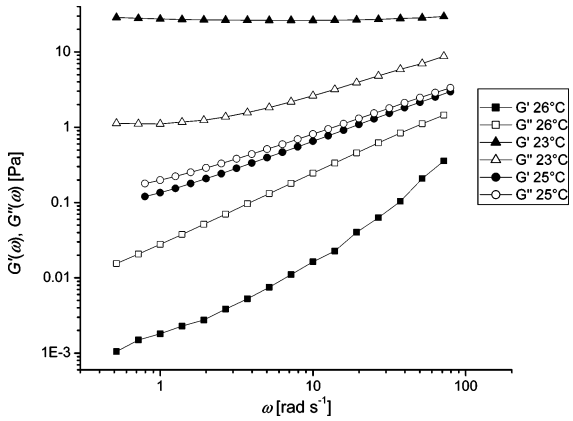

Figure 1. Double-logarithmic plot of the storage ($G'(\omega)$, filled symbols) and loss ($G''(\omega)$, open symbols) shear moduli of the gelatin sample as a function of angular frequency ω at 23 (triangles), 25 (circles), and 26 °C (squares). The regression coefficients for the linear approximations at 25 °C were ≥0.998.

The temperature was varied in steps of 1 K (instrument temperature). After the desired temperature was reached, an equilibration period of 5 min was allowed in each experiment before acquisition was started.

The temperature calibration of the NMR spectrometer was performed in preparatory experiments using a Pt-100 thermocouple mounted to an NMR tube for the determination of the "actual" temperature in the range from 276 to 330 K and compared to the "chemical shift thermometer" using methanol and ethylene glycol.[25] This resulted in a linear relationship of "actual temperature" vs instrument temperature which was used for the correction of the values indicated by the spectrometer. We checked for possible temperature gradients across the sample by placing the thermocouple at the bottom, in the middle, and at the top of the coil region, respectively. For all temperatures used in this study, such differences were less than 0.4 K.

Bruker TOPSPIN 1.3 was used for data acquisition, data processing, and the determination of integrals. The amide region, the aliphatic region, and the most shielded methyl signal were integrated independently. Origin 6.1 was used for the determination of diffusion coefficients using nonlinear regression.

Results and Discussion

To validate our new NMR method, which is based on the diffusion of the gelling agent itself, we first had to measure the gelation point of gelatin with the two most established methods in polymer science, especially for thermoreversible systems:[29] dynamic light scattering (DLS)[30−32] and rheology.[33]

Oscillatory shear rheology experiments were performed. In Figure 1 the frequency dependent storage ($G'(\omega)$) and loss ($G''(\omega)$) moduli for three selected temperatures are shown. The power-law behavior (see eq 1) can be observed at 25 °C with

$$G'(\omega) \propto \omega^{0.71}, \qquad G''(\omega) \propto \omega^{0.65} \tag{1}$$

which is valid for about two decades ($\omega = 0.79-79$ rad s^{-1}).

DLS experiments were performed at a scattering angle of $\theta = 90°$ at several temperatures. Selected time−intensity correlation functions (TCFs) are shown in Figure S1 of the Supporting Information. At 24.5 °C in a delay time window of $t = 0.05-250$ ms a power law

$$g_2(t) - 1 = \frac{\langle I(0)\, I(t)\rangle}{\langle I\rangle^2} - 1 \propto t^{-0.21} \tag{2}$$

was found, where $\langle I(t)\rangle$ is the scattering intensity at time t with respect to $t = 0$ and $\langle I\rangle$ denotes a time average.

Already at temperatures about 0.5 K above and below this gelation threshold the TCFs show solution-like behavior (25 °C) and heterodyne contributions (24 and 23 °C), respectively.

The TCFs could be well described by a Kohlrausch−Williams−Watts[34] stretched exponential function (eq 3):

$$g_2(t) - 1 = A \exp\left[-\left(\frac{t}{\tau}\right)^{\beta}\right] + C \tag{3}$$

where $A \approx 1$ and $C \approx 0$ are constants corresponding to the correlation strength and a very small nonzero plateau as a result of a possible small nonergodic contribution, respectively.

In eq 3 $0 < \beta \leq 1$ is a constant inversely related to the distribution width of the relaxation modes. The parameter τ, together with β, characterizes the mean relaxation time $\langle\tau\rangle$, which is given by

$$\langle\tau\rangle = \int \exp\left[-\left(\frac{t}{\tau}\right)^{\beta}\right] \mathrm{d}t = \left(\frac{\tau}{\beta}\right)\Gamma(\beta^{-1}) \tag{4}$$

where $\Gamma(x)$ depicts the gamma function. The inverse relaxation time is proportional to the translational diffusion coefficient at temperatures above the gel point and to the cooperative diffusion coefficient of the gel mode below the gelation temperature, because the dynamics is then governed by the mesh size of the network. The increase of the relaxation times from 50 to 24.5 °C is a sign of the formation of larger clusters when the gel point is approached. Due to the power-law behavior with no characteristic relaxation time, infinite $\langle\tau\rangle$ can be expected at the gel point, where the translational diffusion coefficient should come to a complete standstill. As the thermoreversible gelation proceeds, the mesh size becomes smaller and the corresponding diffusion is faster, and consequently the relaxation time is decreasing again.[34] Figure 2 exhibits the dependence of the mean relaxation time as a function of temperature. Comparing the positions of the maxima for the cooling (24.5 °C) and heating (29 °C) experiments, a hysteresis is observed.

For the detection of this hysteresis the NMR diffusion measurements were performed both in a cooling regime (53−3 °C) and in a heating regime (3−53 °C). A set of gradient-dependent ^{1}H NMR spectra of the gelatin sample at 53 °C are shown in Figure S2 of the Supporting Information. For data analysis first a simple monoexponential model (eq 5) was applied:

$$I = I_0 \exp\left[-D(\gamma g \delta)^2\left(\Delta - \frac{\delta}{4} - \frac{\tau}{2}\right)\right] + A \tag{5}$$

where I is the measured integral at gradient strength g and γ, Δ, δ, and τ represent the gyromagnetic ratio of protons, the diffusion time, the (total) length of the (bipolar) gradient pulses, and the separation of the gradient pulses of a bipolar pair, respectively. The (hypothetical) integral I_0 at zero gradient strength, the additional intensity contribution A, and the diffusion coefficient D are obtained by nonlinear regression.

Due to heterogeneity in this biopolymer sample, in our experiments we measure diffusion as a sum parameter influenced by individual components, the ratio of which is changing during temperature-dependent measurements. We therefore call these diffusion coefficients, which are obtained by fitting the decay data according to eq 5, "apparent diffusion coefficients".

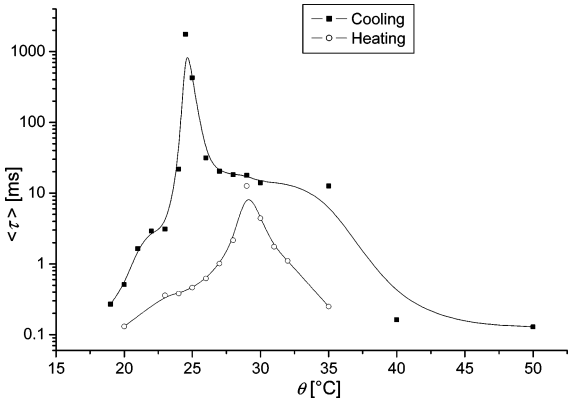

Figure 2. Temperature dependence of the mean relaxation time $\langle\tau\rangle$ determined from the DLS data according to eq 4 during cooling (upper curve) and heating (lower curve). Note that the hysteresis can be recognized from the different positions of the maximum.

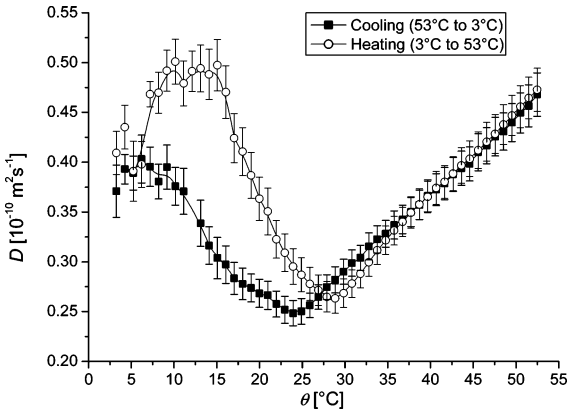

Figure 3. Temperature dependence of the (apparent) diffusion coefficient obtained by fitting the integrals of the most shielded methyl signal to eq 5 for the cooling regime (filled squares) and the heating regime (open circles). The error bars correspond to the statistical error of the diffusion coefficient obtained during the fitting procedure. For the other spectral regions (amide and aliphatic regions) similar behavior was observed.

We are aware of the fact that the apparent diffusion coefficient obtained by fitting to eq 5 depends strongly on the heterogeneity of the sample and on the experimental conditions, e.g., diffusion time. Therefore, this simple model cannot describe the complex behavior of the gelling system exhaustively; especially effects of anomalous diffusion[18] are not considered. However, we are confident enough to use these apparent diffusion coefficients to detect the gelation point as a simple and straightforward method.

The diffusion coefficients obtained by analysis of the data according to eq 5 are depicted in Figure 3. During cooling the apparent diffusion coefficient (D_{app}) reaches a minimum at 24 °C. This can be interpreted as the gelation point and coincides well with the results obtained by rheology (25 °C) and DLS (24.5 °C). As stated above, diffusion is inversely related to the mean relaxation time determined by DLS; thus a minimum at the gel point can be anticipated.

We note that the determination of the gelation temperature can be performed with an accuracy exceeding the temperature steps used (here 1 K) when linear fits to the curves in the region of the gelation point are used, since their intersection marks the gel point.

A possible molecular explanation for the observed increase of D_{app} when cooling below the gel point could be that the molecular weight distribution of the gelatin molecules remaining

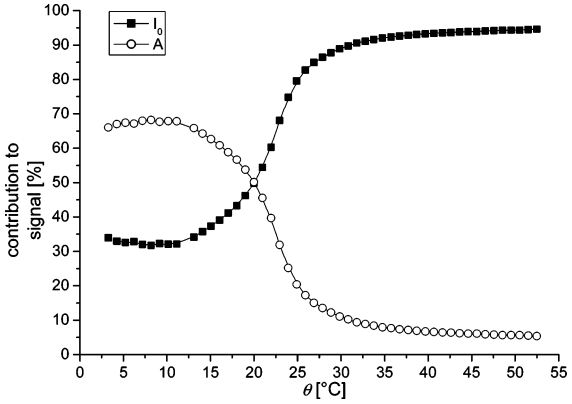

Figure 4. Temperature dependence of the relative contribution of I_0 (filled squares) and A (open circles) (see eq 5) to the observed signal, shown for the fitting results of the most shielded methyl signal during the cooling regime. The values in the diagram are calculated by (100%) $[I_0/(I_0 + A)]$ and (100%)$[A/(I_0 + A)]$, respectively. For the other spectral regions (amide and aliphatic regions) similar behavior was observed.

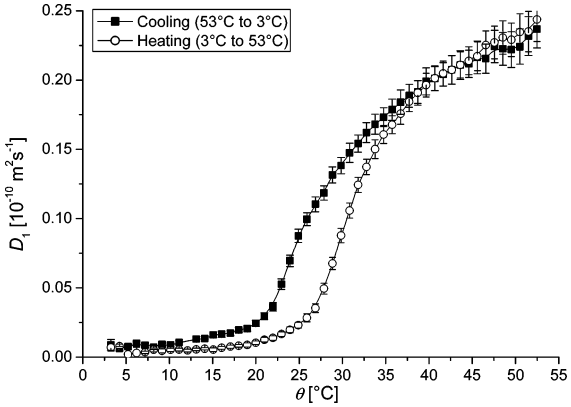

Figure 5. Temperature dependence of the diffusion coefficient D_1 of the network-bound gelatin (slow component) obtained by fitting the integrals of the most shielded methyl signal to eq 6 for the cooling regime (filled squares) and the heating regime (open circles). The error bars correspond to the statistical error of the diffusion coefficient obtained during the fitting procedure.

in the sol is changed systematically. If larger gelatin aggregates have a higher probability to become attached to already formed gel clusters, it is evident that the molecular weight distribution is shifted to smaller aggregates. In this case higher apparent diffusion coefficients will be obtained upon decreasing temperature, since this effect can more than compensate the slight decrease of D with decreasing temperature which is anticipated from the Stokes−Einstein equation. Only for temperatures far below the gel point, when the vast majority of gelatin molecules are attached to the gel, D decreases due to decreasing mesh size of the gelatin network, decreasing temperature, and increasing viscosity.

During heating minimal (apparent) diffusion was obtained at 29 °C (see Figure 3), which is in agreement with DLS measurements performed in a heating regime (see Figure 2). Obviously, the gelation process shows a hysteresis, e.g., already mentioned in ref 3.

Applying linear regression to the regions of the curve surrounding the minimum and interpreting the intercept as the critical temperature yields a gelation point of 24.5 °C for cooling and 28.5 °C for heating.

To obtain deeper insights into the gelation process, we examined the relative contributions of A and I_0 (see eq 5) to the observed signals, which are shown in Figure 4. The qualitative course of these curves resembles titration curves and can be interpreted as an indicator for the presence of two distinct states (or populations) which are interconverted.

Despite its character as a kind of "correction term", A accounts for a considerable part of the signal intensity, especially below the gel point. Therefore, our data suggest the presence of two "components", one diffusing according to the apparent diffusion coefficients shown in Figure 3 and one essentially "nondiffusing".

We interpret these components to be the mobile free gelatin molecules in the sol, which gives rise to the apparent diffusion coefficients plotted in Figure 3, and the network-bound gelatin. When a gel is formed starting from a solution, the (relative) amount of network-bound gelatin increases at the expense of free gelatin, which can easily be recognized in Figure 4. Since bound and free gelatin can exhibit different relaxation times, the molar ratios of both components might differ from the ratio of the signal intensity. However, changes in the molar ratio can still be detected using the NMR signal intensity as an observable. When the relative amount of network-bound gelatin exceeds a certain limit, an infinite percolated cluster can be formed, and the gelation threshold is reached.

Since also the network-bound gelatin should be (slowly) diffusing and therefore exhibit a diffusion coefficient D (slightly) larger than zero, we expanded our model to allow two modes of diffusion (eq 6):

$$I = I_1 \exp\left[-D_1(\gamma g \delta)^2\left(\Delta - \frac{\delta}{4} - \frac{\tau}{2}\right)\right] + I_2 \exp\left[-D_2(\gamma g \delta)^2\left(\Delta - \frac{\delta}{4} - \frac{\tau}{2}\right)\right] \quad (6)$$

where I_1, I_2, D_1, and D_2 are the intensity contributions and diffusion coefficients of the slow component and fast component, respectively; all other symbols have the same meaning as in eq 5.

Although we are aware that biexponential fitting is associated with a variety of problems,[35] especially for "noisy" data, we feel that our data are suited for this model, since no severe baseline problems could be detected, the obtained parameters are reasonable and their trend with changing temperature is continuous.

In Figure 5 the diffusion coefficient of the slow component (D_1 in eq 6) is shown. For temperatures lower than the gelation point this is near zero, since the presence of infinite clusters can be expected. Above the gelation temperature, the diffusion coefficient increases faster (than expected simply by its linear dependence on absolute temperature) since the average size of the clusters decreases dramatically.

The diffusion behavior of the fast component (see Figure S3 of the Supporting Information) also shows a hysteresis and is comparable to the one obtained with monoexponential analysis, since D in eq 5 is most strongly influenced by the fast component. The relative contributions of the slow and fast components to the overall signal during the cooling process is displayed in Figure S4 of the Supporting Information. The share of the slow component increases gradually until gelation starts. After a steep increase its contribution remains rather constant at a higher level once gelation is completed.

The decreasing average size of the clusters can also be seen in Figure 6, where the ratios of both diffusion coefficients obtained according to eq 6 are plotted. This ratio reflects the size difference between free gelatin (fast component) and clusters (slow component). Even high above the gel point this ratio does not approach 1 (but rather 3.5), since there is still a

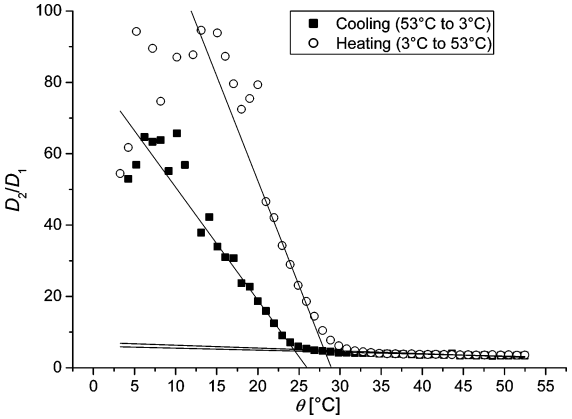

Figure 6. Temperature dependence of the ratio of the diffusion coefficients (D_2/D_1; see eq 6) of the network-bound gelatin (slow component) and the free gelatin (fast component). The solid lines represent the linear regression of the data surrounding the kink. The intercepts of the linear approximations are observed at 24.4 and 28.2 °C for cooling (filled squares) and heating (open circles), respectively.

broad molecular weight distribution including (smaller) clusters as well as individual gelatin molecules. Applying linear fits to the data below and above the gelation temperature, respectively, and subsequent determination of their intersection is another possibility to achieve improved accuracy of the gel point (see Figure 6).

Conclusions

The sol−gel transition of the thermoreversible gelling system of gelatin has been studied by using dynamic light scattering (DLS), oscillatory shear rheology, and for the first time diffusion NMR spectroscopy. NMR diffusion measurements reveal the gel point as a minimum when the apparent diffusion coefficients are plotted vs temperature, and NMR can therefore be used as a simple means to detect this critical threshold in both directions of temperature variation. Deeper understanding of the *full* diffusion curves requires further studies, which are in progress.

Within the experimental errors, all methods result in a gelation temperature of 24−25 °C for the cooling regime. Comparing the heating and cooling regimes, a hysteresis of at least 4 K has been found, which could most easily be studied by the diffusion NMR method.

Acknowledgment. We are grateful to R. Matzker, now at the Institute for Leather and Plastic Sheets (FILK), Freiberg, Germany, for performing some of the DLS measurements. We thank Dr. K. Schröter (Martin Luther University of Halle-Wittenberg, Germany, Experimental Polymer Physics Group) for giving access to the rheometer.

Supporting Information Available: Figure S1 containing seven TCFs measured for the gelatin sample during the cooling regime in the temperature range from 35 to 23 °C. Figure S2 showing an example data set visualizing the diffusional decay as well as the integral regions used. Figure S3 displaying the temperature dependent diffusion behavior of the fast component according to eq 6. Figure S4 visualizing the relative signal contributions of the slow and fast components (see eq 6) for the cooling experiment. This material is available free of charge via the Internet at http://pubs.acs.org.

References and Notes

(1) Guo, L.; Colby, R. H.; Lusignan, C. P.; Whitesides, T. H. *Macromolecules* **2003**, *36*, 9999.
(2) Guo, L.; Colby, R. H.; Lusignan, C. P.; Howe, A. M. *Macromolecules* **2003**, *36*, 10009.
(3) De Carvalho, W.; Djabourov, M. Gelation Under Shear: A Dynamic Phase Transition. In *The Wiley Polymer Networks Group Review Series*; te Nijenhuis, K., Mijs, W. J., Eds.; John Wiley & Sons Ltd.: New York, 1998; Vol. 1, pp 91−106.
(4) Blanco, M. C.; Leisner, D.; Vázquez, C.; López-Quintela, M. A. *Langmuir* **2000**, *16*, 8585.
(5) Okamoto, M.; Norisuye, T.; Shibayama, M. *Macromolecules* **2001**, *34*, 8496.
(6) Sharma, J.; Bohidar, H. B. *Colloid Polym. Sci.* **2000**, *278*, 15.
(7) Bohidar, H. B.; Jena, S. S. *J. Chem. Phys.* **1994**, *100*, 6888.
(8) Bohidar, H. B.; Jena, S. S. *J. Chem. Phys.* **1993**, *98*, 8970.
(9) Joly-Duhamel, C.; Hellio, D.; Ajdari, A.; Djabourov, M. *Langmuir* **2002**, *18*, 7158.
(10) Joly-Duhamel, C.; Hellio, D.; Djabourov, M. *Langmuir* **2002**, *18*, 7208.
(11) te Nijenhuis, K. *Adv. Polym. Sci.* **1997**, *130*, 160.
(12) Morris, G. A. *Encycl. Nucl. Magn. Reson.* **2002**, *9*, 35.
(13) Morris, G. A.; Barjat, H. *Anal. Spectrosc. Lib.* **1997**, *8*, 209, 211.
(14) Pregosin, P. S.; Kumar, P. G. A.; Fernandez, I. *Chem. Rev.* **2005**, *105*, 2977.
(15) Pregosin, P. S.; Martinez-Viviente, E.; Kumar, P. G. A. *Dalton Trans.* **2003**, *21*, 4007.
(16) Brand, T.; Cabrita, E. J.; Berger, S. *Prog. Nucl. Magn. Reson. Spectrosc.* **2005**, *46*, 159.
(17) Cohen, Y.; Avram, L.; Frish, L. *Angew. Chem.* **2005**, *117*, 524.
(18) Walderhaug, H.; Nyström, B. *J. Phys. Chem. B* **1997**, *101*, 1524.
(19) Ren, S. Z.; Shi, W. F.; Zhang, W. B.; Sorensen, C. M. *Phys. Rev. A* **1992**, *45*, 2416.
(20) Richter, S.; Brand, T.; Berger, S. *Macromol. Rapid Commun.* **2005**, *26*, 548.
(21) Abe, K.; Matsukawa, S.; Abe, M.; Watanabe, T. *Trans. Mater. Res. Soc. Jpn.* **2001**, *26*, 589.
(22) Traoré, A.; Foucat, L.; Renou, J.-P. *Eur. Biophys. J.* **2000**, *29*, 159.
(23) Kjøniksen, A.-L.; Hiorth, M.; Roots, J.; Nyström, B. *J. Phys. Chem. B* **2003**, *107*, 6324.
(24) Wu, D.; Chen, A.; Johnson, C. S., Jr. *J. Magn. Reson. A* **1995**, *115*, 260.
(25) Berger, S.; Braun, S. *200 and More NMR Experiments, A Practical Course*; Wiley-VCH: Weinheim, 2005; pp 141−148, 455.
(26) Damberg, P.; Jarvet, J.; Gräslund, A. *J. Magn. Reson.* **2001**, *148*, 343.
(27) Mills, R. *J. Phys. Chem.* **1973**, *77*, 685.
(28) Meiboom, S.; Gill, D. *Rev. Sci. Instrum.* **1958**, *29*, 688.
(29) Richter, S.; Matzker, R.; Schröter, K. *Macromol. Rapid Commun.* **2005**, *26*, 1626.
(30) Geissler, E. Dynamic Light Scattering from Polymer Gels. In *Dynamic Light Scattering*; Brown, W., Ed.; Clarendon Press: Oxford, 1993; pp 471−511.
(31) Martin, J. E.; Adolf, D. *Annu. Rev. Phys. Chem.* **1991**, *42*, 311.
(32) Shibayama, M.; Norisuye, T. *Bull. Chem. Soc. Jpn.* **2002**, *75*, 641.
(33) Winter, H. H.; Mours, M. *Adv. Polym. Sci.* **1997**, *134*, 165.
(34) Rodd, A. B.; Dunstan, D. E.; Boger, D. V.; Schmidt, J.; Burchard, W. *Macromolecules* **2001**, *34*, 3339.
(35) Istratov, A. A.; Vyvenko, O. F. *Rev. Sci. Instrum.* **1999**, *70*, 1233.